polycyclic enones such as testosterone.

Torsional distortions in the $^3\pi\pi^*$ state of α,β-enones have been claimed to be a major deactivation pathway leading to disappearance of phosphorescence.[41] Tentatively, we suggest that the spectroscopic triplet state is separated from the relaxed one(s) observed at room temperature by an energy barrier. In the monocyclic enones studied by Yamauchi et al.,[38] the barrier then should be very low. In two bicyclic α,β-enones (in which the double bond is common to both rings) the study of the temperature and viscosity dependence of ϕ_P has led[22] to the conclusion that the barrier is predominantly viscosity-induced. Our experiments on the temperature dependence of ϕ_P of the enones also indicate the existence of a barrier. Interestingly, the fact that $\phi_P(T)$ of **2a** in EPA and in the much more viscous glycerol are about equal shows the absence of a viscosity effect and suggests that the barrier is of intrinsic nature.

Concluding Remarks

CPP turns out to be a useful technique to distinguish $^3\pi\pi^*$ from $^3n\pi^*$ states, and it supplements the arsenal of already existing techniques. It is gratifying that the inherent sensitivity of optical activity toward molecular structure—long exploited to probe ground-state conformation and, more recently, the geometry of the lowest excited singlet state[42]—can also be used to study the phosphorescent triplet state.

In view of the many approximations used, our explanation of the CPP data of α,β-enones is tentative and further investigations should be made. An essential feature of our model is the strong dependence of g_{lum} on the magnitude of the T-T gap and on the twist in the chromophore. It would be interesting to study the relationship quantitatively with enones that are more rigid and have larger angles of twist than the compounds described here.

The enhancement of optical activity by T-T coupling opens other interesting possibilities. For instance, the mere fact that g_{lum} values of $^3\pi\pi^*$ phosphorescences can be very high can be exploited in the study of racemization rates[43] and energy-transfer processes[44] in the triplet state.

Further, in the $^3\pi\pi^*$ state a planar α,β-unsaturated ketone with a very small T-T gap might adopt a twisted conformation due to the pseudo-Jahn-Teller effect. One of the enantiomeric twisted conformers might be stabilized in a chiral solvent.

Acknowledgment. We thank J. Cornelisse for his interest in this work. This research was supported by The Netherlands Foundation for Chemical Research (SON) with financial aid from The Netherlands Organization for Scientific Research (NWO).

Registry No. **1a**, 63975-59-7; **1b**, 4087-39-2; **2a**, 58-22-0; **2b**, 1045-69-8; **2c**, 57-83-0; **2d**, 601-57-0; **3**, 71-58-9; **4**, 604-26-2; **5**, 1923-21-3; **6**, 3702-37-2; **7a**, 434-22-0; **7b**, 1425-10-1; **8**, 51-98-9; **9a**, 571-41-5; **9b**, 3986-85-4; **10**, 571-45-9; **11**, 897-03-0; **12**, 988-19-2; **13**, 1449-05-4; **14**, 130798-68-4; **15**, 979-02-2; **16**, 982-06-9.

(41) Cargill, R. L.; Bundy, W. A.; Pond, D. M.; Sears, A. B. *Mol. Photochem.* **1971**, *3*, 123-139.
(42) See, e.g.: Schippers, P. H.; van der Ploeg, J. P. M.; Dekkers, H. P. J. M. *J. Am. Chem. Soc.* **1983**, *105*, 84-89 and ref 1.
(43) Analogous to those in the $^1n\pi^*$ states of ketones, studied via the circular polarization of the fluorescence, see: Schippers, P. H.; Dekkers, H. P. J. M. *Chem. Phys. Lett.* **1982**, *88*, 512-516. Dekkers, H. P. J. M.; Moraal, P. F. In *Proceedings of the First International Conference on Circular Dichroism*; Bulgarian Academy of Sciences: Sofia, 1985; pp 322-326. Very recently, the use of the time-resolved CPL technique in the study of the excited-state racemization kinetics of labile lanthanide complexes was reported: Metcalf, D. H.; Snyder, S. W.; Demas, J. N.; Richardson, F. S. *J. Am. Chem. Soc.* **1990**, *112*, 469-479.
(44) Rexwinkel, R. B.; Dekkers, H. P. J. M. Unpublished results.

Examination of Allyl Radical Excited-State Dynamics and Ground-State Vibrational Frequencies by Ultraviolet Resonance Raman Spectroscopy

James D. Getty, Martin J. Burmeister, Sjon G. Westre, and Peter B. Kelly*

Contribution from the Department of Chemistry, University of California, Davis, California 95616. *Received July 2, 1990. Revised Manuscript Received September 24, 1990*

Abstract: The first Raman spectra of the allyl radical have been obtained. The intensities of the observed Raman spectra indicate excited-state dynamics consistent with a disrotary photoisomerization of the allyl radical to form a cyclopropyl radical. Prior to this work, direct examination of the photoisomerization pathway was not possible due to limitations of the techniques applied. The ground-state vibrational frequencies observed are found to be in excellent agreement with recent theoretical calculations suggesting a reassignment of the literature infrared frequencies. This work demonstrates that resonance Raman spectroscopy is a powerful method for examination of gas-phase free radicals.

Introduction

The allyl radical is the simplest conjugated hydrocarbon radical. It is an important intermediate in many photochemical reactions and a proposed intermediate for soot formation in hydrocarbon combustion.[1] Though numerous theoretical[2-4] and experimental investigations[5-11] have been performed on the allyl radical, there remain several discrepancies between the experimental and theoretical ground-state frequencies for this system. The ground-state vibrational frequencies of the allyl radical have been experimentally examined by Oakes and Ellison,[5] Maier et al.,[6] Sappey and Weishaar,[7] and Hudgens and Dulcey.[8] Maier and co-workers utilized matrix isolation techniques to obtain the infrared spectra of the allyl radical. However, Maier et al. had difficulties assigning their matrix spectra due to spectral congestion and overlapping bands from secondary photoproducts. Sappey and Weishaar[7]

(1) Weissman, M.; Benson, S. W. *Prog. Energy Combust. Sci.* **1989**, *15*, 273.
(2) Takada, T.; Dupuis, M. *J. Am. Chem. Soc.* **1983**, *105*, 1713.
(3) Ystenes, M.; Fjorstad, E. *Spectrochim. Acta, A*, in press.
(4) Ha, T. K.; Baumann, H.; Oth, J. F. M. *J. Chem. Phys.* **1986**, *85*, 1438.
(5) Oakes, J. M.; Ellison, G. B. *J. Am. Chem. Soc.* **1984**, *106*, 7734.
(6) Maier, G.; Reisenauer, H. P.; Rohde, B.; Dehnicke, K. *Chem. Ber.* **1983**, *116*, 732.
(7) Sappey, A. D.; Weishaar, J. C. *J. Phys. Chem.* **1987**, *91*, 3731.
(8) Hudgens, J. W.; Dulcey, C. S. *J. Phys. Chem.* **1985**, *89*, 1505.
(9) Callear, A. B.; Lee, H. K. *Trans. Faraday Soc.* **1968**, *64*, 308.
(10) Nakashima, N.; Yoshihara, K. *Laser Chem.* **1987**, *7*, 177.
(11) Ramsay, D. A. In *Vibrational Spectra and Structure*; Durig, J. R., Ed.; Elsevier: New York, 1985; Vol. 14.

0002-7863/91/1513-801$02.50/0

obtained the multiphoton ionization spectrum of the allyl radical which they generated by gas-phase flash photolysis. The $\tilde{1}\ ^2B_1 \leftarrow \tilde{X}\ ^2A_2$ transition at 405 nm was used to enhance the multiphoton ionization process. By analyzing the vibronic features observed in their flash photolysis absorption spectrum, Sappey and Weishaar were able to assign three of the ground-state vibrational frequencies. Oakes and Ellison observed vibrational structure of the allyl radical by photoelectron spectroscopy of the allylic anion.[5] Multiple photon ionization spectra of the deuterated allyl radical have also been obtained by Hudgens and Dulcey.[8]

Theoretical calculations of the ground-state vibrational frequencies were performed by Takada and Dupuis[2] as well as Ystenes and Fjorstad.[3] Both of these studies used ab initio multiconfigurational Hartree–Fock methods. The two theoretical studies agree very well with each other but disagree with the assigned experimental frequencies of Maier et al.

The far-ultraviolet absorption spectrum of the allyl radical was first recorded by Callear and Lee.[9] Their spectra of the $\tilde{2}\ ^2B_1 \leftarrow \tilde{X}\ ^2A_2$ transition showed discrete vibrational structure; however, no vibrational analysis of the spectrum was presented. Nakashima and Yoshihara also recorded the absorption spectrum of the $\tilde{2}\ ^2B_1 \leftarrow \tilde{X}\ ^2A_2$ transition and demonstrated that vibrationally hot radicals formed by photolysis of allyl halides were rapidly cooled by addition of an atmosphere of nitrogen buffer gas.[10]

Ab initio calculations of the excited states of the allyl radical have been performed by several groups.[4,12,13] Ha et al. found that the $\tilde{2}\ ^2B_1$ state observed at 224 nm is actually a mixture of B_1 reference configurations with the largest contribution from the $...(6a_1)^2\ (4b_2)^2(1b_1)^2(2b_1)^1$ configuration.[4] Less extensive SCF CI studies by Merlet et al.[12] and Farnell and Richards[13] considered the allyl–cyclopropyl isomerization. Placement of the odd electron in the $1a_2$ molecular orbital correlates with the ground state of the allyl radical, while occupation of the $2b_1$ molecular orbital by the odd electron correlates with the ground state of the cyclopropyl radical.[12,13] Both theoretical studies found that the photochemical isomerization of the allyl radical resulting from excitation of the unpaired electron from the $1a_2$ molecular orbital to the $2b_1$ molecular orbital favors the disrotary pathway on the excited-state surface.[12,13]

Time-resolved resonance Raman spectroscopy is a general method for examination of gas-phase transient species. Reviews by Foster and Miller,[14] and Ramsay[11] highlight the tremendous opportunities for increased understanding of the spectra and structure of free radicals. Characteristics of the excited-state surface and predissociation dynamics of the methyl radical Rydberg 3s state have been examined by using resonance Raman spectroscopy. The selectivity and sensitivity of the technique have been demonstrated in the study of higher vibration levels of CH_3 and CD_3.[15,16] In this paper the ground-state vibrational structure and the excited-state dynamics of the allyl radical will be examined by using resonance Raman spectroscopy.

Experimental Section

The resonance Raman/photolysis system used to examine gas-phase free radicals is based on a 20-Hz Nd:YAG laser and dye laser. The gas-phase allyl radical was produced by photolysis of allyl iodide with the fourth harmonic of the Nd:YAG laser. Allyl bromide photolyzed with the fifth harmonic of the Nd:YAG laser was used as an additional method of generating the allyl radical. The fifth harmonic radiation was generated by sum frequency mixing of the fourth harmonic with the fundamental of the Nd:YAG in β barium borate.[15,17] Both precursors yielded the same spectra of the radical.

The Raman probe laser was tuned to the allyl $\tilde{2}\ ^2B_1 \leftarrow \tilde{X}\ ^2A_2$ transition at 224.63 nm. The tuneable far-ultraviolet radiation was produced by frequency doubling the output of a DCM/LDS 698 dye laser in KD*P

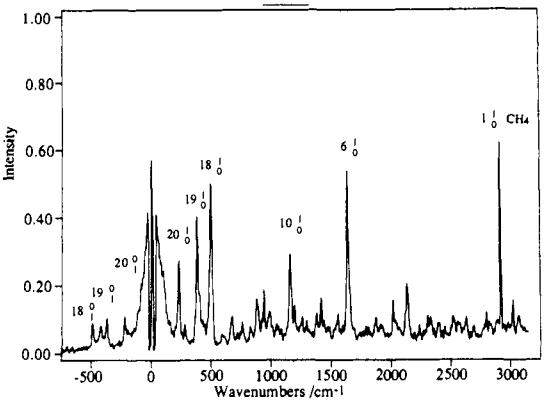

Figure 1. Resonance Raman spectrum of allyl iodide excited at 224.63 nm. The relative intensity is scaled to the methane buffer gas signal at 2917 cm^{-1}.

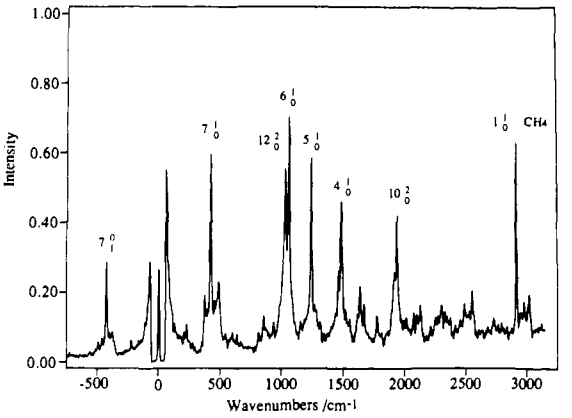

Figure 2. Allyl radical Raman spectrum excited at 224.63 nm. The intensities are shown relative to the methane signal at 2917 cm^{-1}.

followed by sum frequency mixing the second harmonic with the fundamental with β barium borate. The resulting 224.63-nm radiation was separated from the 336.8- and 673.5-nm radiation by use of SI-UV quartz prisms. The probe beam was directed to the sample area and delayed 15 ns relative to the photolysis pulse. The sample flow consisted of 10 Torr of allyl iodide and 750 Torr of methane. The extent of photolysis of the precursor was determined by comparison of the intensity of the allyl iodide 6_0^1 Raman band at 1637 cm^{-1} with and without photolysis. The Raman scattered light was collected in backscatter geometry by a 2-in.-diameter $f/0.67$ spherical mirror and focused onto the slits of a 1-m Czerny-Turner monochromator. Spectra of the gas-phase radical were recorded by using a solar blind Hamamatsu R166UH photomultiplier tube and gated integrator. The output was sampled by an A/D convertor and stored on an IBM PC/AT computer.

Results

Allyl iodide and allyl bromide were used as precursors for the allyl radical. Allyl iodide produced Raman spectra of the radical with better signal to noise ratios than allyl bromide. However, the allyl iodide Raman spectrum was enhanced with 224.63-nm excitation due to resonance with the $\pi^* \leftarrow \pi$ transition which complicated the analysis of the radical spectrum. The resonance Raman spectrum of allyl iodide is shown in Figure 1. Frequencies were assigned in accord with the Raman and infrared work of McLachlan and Nyquist.[18]

The spectrum in Figure 2 was generated by using 0.2 mJ/pulse of 224.63-nm light for Raman excitation and 5 mJ/pulse of 266-nm radiation which photolyzed 54% of the allyl iodide precursor. Using the recombination rate[19] of van den Bergh and Callear yields an estimated 5.0 Torr of allyl radical present 15 ns following photolysis. The 1,5-hexadiene recombination product was not observed in the Raman spectrum due to its low concen-

(12) Merlet, P.; Peyerimhoff, S. D.; Buenker, R. J.; Shih, S. *J. Am. Chem. Soc.* **1974**, *96*, 959.
(13) Farnell, L.; Richards, W. G. *J. Chem. Soc., Chem. Commun.* **1973**, 334.
(14) Foster, S. C.; Miller, T. A. *J. Phys. Chem.* **1989**, *93*, 5986.
(15) Kelly, P. B.; Westre, S. G. *Chem. Phys. Lett.* **1988**, *151*, 253.
(16) Westre, S. G.; Kelly, P. B. *J. Chem. Phys.* **1989**, *90*, 6977.
(17) Hudson, B. *Spectroscopy* **1987**, *2*, 33.
(18) McLachlan, R. D.; Nyquist, R. A. *Spectrochim. Acta* **1968**, *24A*, 103.
(19) van den Bergh, H. E.; Callear, A. B. *Trans. Faraday Soc.* **1970**, *66*, 2681.

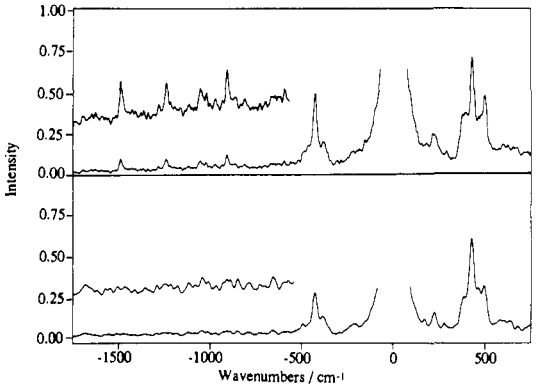

Figure 3. Resonance Raman spectra of the allyl radical produced from 266-nm photolysis of allyl iodide. The lower trace was recorded with methane as a buffer gas and a 15-ns delay between arrival of photolysis and probe pulses. The upper trace was generated by using argon as a buffer gas. The insert traces are 3× expansions of the anti-Stokes spectral region showing the appearance of vibrationally hot allyl radical with argon buffer gas.

tration and lack of resonance enhancement at 224.63 nm.

One of the problems that arises in gas-phase photolysis experiments is spectral congestion. When a radical is formed by photodissociation, it may have a significant amount of vibrational and rotational energy. Vibrational excitation can result in hot bands that complicate the observed spectrum. Rotational excitation broadens the vibrational features and limits the attainable resolution. To alleviate these problems, the resonance Raman spectra are generally taken with a 15-ns delay between photolysis and probe pulses with 750 Torr of buffer gas to allow vibrational and rotational relaxation of the radical. However, not all buffer gases will fully relax the radical in 15 ns.

The upper trace of Figure 3 was generated by using argon as a buffer gas. The significant intensity in the anti-Stokes spectrum is due to the poor efficiency of argon at thermalizing the allyl radical. The lower trace was generated with methane as a buffer gas and the same delay between the arrival of the photolysis and probe pulses. While the radical may not be completely cooled to room temperature, the anti-Stokes spectrum indicates that only the lowest frequency vibration has retained a significant population. Thus, by judicious choice of buffer gas and delay time, the spectral congestion due to hot bands can be minimized.

The spectral resolution in Figure 2 was 11 cm^{-1} with ± 4 cm^{-1} standard deviation in determining the line center of the spectral features. Six prominent features at 429, 1035, 1068, 1246, 1487, and 1932 cm^{-1} appeared upon photolysis of allyl iodide and grew linearly with increased photolysis power, indicating that these features are due to a one photon primary photolysis product. Infrared[6] and ESR[20] spectroscopies have demonstrated that allyl halides yield the allyl radical as the primary photolysis product.

Discussion

The assignment of the allyl radical Raman spectrum was based on the ab initio calculations of Takada and Dupuis[2] and Ystenes and Fjorstad.[3] The two theoretical studies yield comparable values for the vibrational frequencies. The scaled frequencies of Ystenes and Fjorstad are given in Table I. The most intense bands in the Raman spectrum are due to the fundamentals of totally symmetric vibrations. The even overtones of non totally symmetric vibrations that have large changes in the force constant on the excited-state surface also appear in the Raman spectrum.[21] The assumption that the strongest bands in the Raman spectrum are totally symmetric normal modes yields the assignment of the 429-, 1246-, and 1487-cm^{-1} bands as ν_7, ν_5, and ν_4. This is in excellent agreement with the ab initio frequencies. The original work of

Table I. Vibrational Frequencies of the Allyl Radical (cm^{-1})

	assignment	scaled ab initio calcn[3]	IR matrix[6]	MPI spectra[7]	this work
a_1					
ν_1	asym CH_2 stretch (sym)	3109	3105	–	–
ν_2	CH stretch	3028	3048	–	–
ν_3	sym CH_2 stretch (sym)	3013	3016	–	–
ν_4	CH_2 scissors (sym)	1484	1477[a]	–	1487
ν_5	CH_2 rock (sym)	1245	1242[a]	–	1246
ν_6	CCC stretch (sym)	1017	–[a]	–	1068
ν_7	CCC bend	416	–[a]	426	429
a_2					
ν_8	CH_2 out of plane bend (asym)	779	–	–	–
ν_9	CH_2 twist (asym)	538	–	558	–
b_1					
ν_{10}	CH out of plane bend	979	985	–	overtone 1936
ν_{11}	CH_2 out of plane bend (sym)	805	802	–	–
ν_{12}	CH_2 twist (sym)	521	511[a]	508	overtone 1035
b_2					
ν_{13}	CH_2 stretch (asym)	3105	3105	–	–
ν_{14}	CH stretch (asym)	3015	3016	–	–
ν_{15}	CH_2 scissors (asym)	1490	1463	–	–
ν_{16}	CH bend	1404	1389[a]	–	–
ν_{17}	CCC stretch (asym)	1215	–[a]	–	–
ν_{18}	CH_2 rock (asym)	919	–[a]	–	–

[a] Reassigned as suggested in ref 3.

Maier and co-workers assigned the 511-cm^{-1} IR band as ν_7. Lack of a Raman band at 511 cm^{-1} strongly supports the reassignment of this IR band to ν_{12} as suggested by Ystenes and Fjorstad. The only reasonable possibility for the 1936-cm^{-1} band is the even overtone of the CH out of plane bend $2\nu_{10}$. Using the relation

$$10_0^2 - 2 \times 10_0^1 = 2\chi_{10,10} \quad (1)$$

and substituting in the observed infrared matrix value[6] for 10_0^1 yield an estimate of $\chi_{10,10} = -17$ cm^{-1}, which is in the range expected for this type of normal mode. The value for $\chi_{10,10}$ is not exact since the matrix effects on the fundamental frequency are not known.

Our assignment of the 1035-cm^{-1} band as $2\nu_{12}$ and the 1068-cm^{-1} band as ν_6 are tentative but are based on several observations. From calculated frequencies, there are three possibilities for the assignment of these two bands: ν_6, $2\nu_9$, and $2\nu_{12}$. Sappey and Weishaar's observation[7] of the C–C torsion vibration ν_9 at 558 cm^{-1} makes it unlikely that our observed band at 1068 cm^{-1} is $2\nu_9$. The assignment of the 1068-cm^{-1} band as $2\nu_9$ would require $\chi_{9,9} = -24$ cm^{-1}. Since the potential for ν_9 is expected to be sinusoidal like the torsion potential in ethylene, where the anharmonic constant of the torsion vibration[22] is ~ -1.3 cm^{-1}, an anharmonic constant of -24 cm^{-1} in unreasonable. Taking the MPI value[7] of 508 cm^{-1} for ν_{12} and using our 1035-cm^{-1} band assignment for $2\nu_{12}$ yield an estimate for $\chi_{12,12}$ of $\sim +9.5$ cm^{-1}. This value is in better agreement with the anharmonic constant expected for a torsion vibration. Determination of the gas-phase frequency for ν_{12} by infrared spectroscopy will yield a better value for $\chi_{12,12}$.

Callear and Lee report a structured UV absorption spectrum with many bands.[9] There is not an obvious assignment of the observed spectrum, but there are repeated differences of 430, 1065, and 1255 cm^{-1} between several of the observed absorption bands on the low-energy side of the absorption maximum. These particular differences are noted because they correspond to the observed a_1 vibrations in the resonance Raman spectrum. Generally, electronic absorption bands that appear on the low-energy side of the electronic band origin originate from vibrationally hot levels

(20) Sears, T. S.; Volman, D. H. *J. Photochem.* **1984**, *26*, 85.
(21) Hudson, B.; Kelly, P. B.; Ziegler, L. D.; Desiderio, R. A.; Gerrity, D. P.; Hess, W.; Bates, R. In *Advances in Laser Spectroscopy*; Garetz, B. A., Lombardi, J. R., Eds.: Heyden: Philadelphia, 1986.
(22) Sension, R. J.; Mayne, L.; Hudson, B. *J. Am. Chem. Soc.* **1987**, *109*, 5036.

of the ground state. The observation of a 1065-cm^{-1} difference between hot band absorption features supports the assignment of our observed 1068-cm^{-1} Raman band as the fundamental of ν_6. Differences corresponding to non totally symmetric normal modes do not normally appear in the electronic absorption hot band spectra. Vibronic coupling of the type seen in benzene would be required for fundamentals of non totally symmetric modes to appear as differences between hot hand absorption features.[23]

The alternative assignment of the 1035-cm^{-1} band to ν_6 and the 1068-cm^{-1} band to $2\nu_{12}$ cannot be excluded from consideration. Examination of the allyl-d_5 radical spectrum will aid in definitive assignment of these bands. Since both ν_6 and $2\nu_{12}$ levels are of a_1 symmetry and twice the experimental value for ν_{12} coincides with the theoretical value for ν_6, there is a strong possibility for a Fermi resonance interaction between these two levels.

The infrared absorption data of Maier et al.[6] in Table I have been reassigned as recommended by Ystenes and Fjorstad.[3] This reassignment is based on the calculated infrared intensities.[3] The agreement of our results with the literature experimental values[6,7] shown in Table I and with the scaled ab initio frequencies of Ystenes and Fjorstad is quite good. The ab initio frequencies of Takada and Dupuis[2] are also in good agreement when proper scaling is taken into consideration. The multiphoton ionization experiments by Hudgens et al. found several vibrational hot bands.[8] The only identifiable frequency from their work is the band at 413 ± 30 cm^{-1}, which is ν_7. The other vibrations are difficult to identify due to the relatively large error limits. Their band at 343 ± 30 cm^{-1} in the allyl-d_5 spectrum is in good agreement with the calculated value,[2] less 10% for scaling, of ν_7 for the deuterated radical.

The intensities of normal modes in the resonance Raman spectra are indicative of the geometry changes on the excited-state surface. The factors that determine the intensity of resonance Raman scattering can be described by using either the Kramers–Heisenberg–Dirac formalism[21,24,25] or the time-dependent wavepacket formalism.[26-28] In either formalism, the intensity of the Raman scattering from vibronic state gm to state gn is given by

$$I_{mn} \propto \nu_0 (\nu_0 - \nu_{mn})^3 |\alpha_{mn}|^2 \qquad (2)$$

where ν_0 is the frequency of the laser, ν_{mn} is the energy difference between states gm and gn, and α_{mn} is the transition polarizability. The Kramers–Heisenberg–Dirac dispersion equation for Raman amplitude gives the excitation wavelength dependence of α_{mn} in terms of a summation over states. When the energy of the incident photons matches that of a single allowed electronic transition, the expression simplifies, yielding the resonant term with a summation over vibronic levels of the excited state

$$\alpha_{mn} = \sum_v \frac{\langle g|\mu_\rho|e\rangle\langle e|\mu_\sigma|g\rangle\langle m|v\rangle\langle v|n\rangle}{h\nu_{ev} - h\nu_0 + i\Gamma} \qquad (3)$$

where g and e denote the ground and intermediate excited electronic states, μ is the electronic transition dipole operator, and σ and ρ indicate the polarization direction. The initial, intermediate, and final vibrational levels are m, v and n, respectively. The energy and dephasing of the intermediate state are given by $h\nu_{ev}$ and Γ.

Examination of eq 3 shows that the Raman scattering amplitude depends on the energy denominator, the electronic transition moments, and the vibrational overlap integrals. For our experiment, the laser was tuned into resonance with the apparent vibronic band origin at 224.63 nm. The nonvibrating excited-state level was the largest component in the summation. While the energy differences in the denominator and the electronic transition integrals are important components of the intensity determination, the vibrational integrals will determine the relative strength of the vibrational bands that appear in the Raman spectrum. The vibrational integrals are very sensitive to changes in the excited-state surface relative to the ground-state surface.

A shift in the position of the minimum of the potential energy curve is a displacement for a totally symmetric normal mode. A displacement or large force constant change in the excited-state potential energy curve relative to the ground-state potential energy curve yields resonance enhancement in the fundamental and overtones for totally symmetric vibrations. An excited state potential that is directly dissociative along a totally symmetric normal coordinate will result in strong resonance Raman scattering to the fundamental and overtones for the normal mode involved.[29] A force constant change or a dissociation involving a non totally symmetric normal mode will yield intensity in even overtones of the non totally symmetric normal mode.[21]

Lack of intensity in a normal mode in the resonance Raman spectrum also can be used to describe the excited-state surface. Identical potential surfaces for ground and excited states yield Franck–Condon factors that contribute only to resonant Rayleigh and pure rotational Raman scattering; therefore, normal modes that are not displaced and do not have a force constant change will not be active in the resonance Raman spectrum.

Resonance Raman spectroscopy is sensitive only to the portion of the excited-state potential directly accessed by a vertical transition from the ground state. Displacements that occur in the exit channel of an isomerization or photodissociation will not contribute to a resonance Raman spectrum. Dissociations that occur after relaxation to a different excited-state surface will not influence the spectrum either.

Several totally symmetric normal mode fundamentals and overtones of non totally symmetric normal modes appear in the resonance Raman spectrum at 224.63 nm (Figure 2). Our results are in qualitative agreement with the theoretically predicted disrotary photoisomerization of allyl to cyclopropyl radical.[12,13] The calculated Walsh diagram shows that promotion of the electron from the $1a_2$ (π_2) nonbonding molecular orbital to the $2b_1$ (π_3) antibonding molecular orbital causes a decrease in the CCC bonding for the excited state.[30] The observation of significant activity in ν_7 is in agreement with a decrease of the CCC bond angle on the excited-state surface. The excited-state character of the hybridization on the central carbon is expected to be less sp^2 hybrid and more sp^3 hybrid than that of the ground state to account for the decrease in the CCC bond angle. The strong activity in $2\nu_{10}$, the out of plane bend for the hydrogen on the central carbon, supports the proposed shift in hybridization. The large intensity in the terminal CH_2 b_1 torsion, the $2\nu_{12}$ feature, strongly supports the hypothesis of the disrotary pathway for the isomerization.[11,12] The unusually large intensity in $2\nu_{12}$ and $2\nu_{10}$ shows that there are strong forces along both coordinates in the photoisomerization process. The 1.39-Å CC bond length in allyl[2] is shorter than the 1.48-Å CC bond length in the cyclopropyl radical.[31] This results in a displacement for ν_6 on the excited-state surface, yielding the observed intensity in ν_6 in the resonance Raman spectrum. Activity in ν_4 and ν_5 is consistent with a rehybridization of the terminal carbons and motion of the hydrogens from planar to tetrahedral coordination. The complete absence of fluorescence from the $\tilde{2}\ ^2B_1$ state is consistent with the proposed rapid photoisomerization. At large nuclear displacements the $\tilde{2}\ ^2B_1$ excited-state surface may mix with the $\tilde{1}\ ^2B_1$ surface; however, our experiments are not sensitive to such an interaction in the isomerization exit channel.

The $\tilde{2}\ ^2B_1$ state has sufficient energy to dissociate to yield a hydrogen atom and allene as has been suggested for the lower lying $\tilde{1}\ ^2B_1$ state.[32] However, direct photodissociation of the central

(23) Ziegler, L. D.; Hudson, B. *Excited States* **1982**, *5*, 41.
(24) Tang, J.; Albrecht, A. C. In *Raman Spectroscopy*; Szymanski, H., Ed.; Plenum: New York, 1970; Vol. 2, p 33.
(25) Lee, D.; Albrecht, A. C. In *Advances in Infrared and Raman Spectroscopy*; Clark, R. J. H., Hester, R. E., Eds.; Wiley: New York, 1985; Vol. 12, p 179.
(26) Tannor, D.; Heller, E. J. *J. Chem. Phys.* **1982**, *77*, 202.
(27) Myers, A. B.; Mathies, R. A.; Tannor, D. J.; Heller, E. J. *J. Chem. Phys.* **1982**, *77*, 3857.
(28) Shin, K. S. K.; Zink, J. I. *Inorg. Chem.* **1989**, *28*, 4358.
(29) Imre, D.; Kinsey, J.; Sinha, A.; Krenos, J. *J. Phys. Chem.* **1984**, *88*, 3956.
(30) Boerth, D. W.; Streitwieser, A. *J. Am. Chem. Soc.* **1978**, *100*, 750.
(31) Dupuis, M.; Pacansky, J. *J. Chem. Phys.* **1982**, *72*, 2511.
(32) Currie, C. L.; Ramsey, D. A. *J. Chem. Phys.* **1966**, *45*, 488.

CH bond on the $\tilde{2}\ ^2B_1$ surface is not supported by the resonance Raman intensities or theoretical results. The direct photodissociation would yield strong intensity in ν_2, the CH stretch. The Raman bands at 2917 and 3020 cm^{-1} in Figure 3 are due to the methane buffer gas. No strong Raman bands in the CH stretch region are observed when argon is used as a buffer gas. The terminal CH_2 groups would rotate to the perpendicular geometry of allene corresponding to motion in the ν_9 coordinate of the allyl radical, giving rise to $2\nu_9$ in the Raman spectrum. Neither of these features appears in the Raman spectrum resonantly enhanced by the $\tilde{2}\ ^2B_1$ state.

Conclusions

Examination of the allyl radical by resonance Raman spectroscopy has shown that the literature infrared frequencies should be reassigned and that the ab initio theoretical frequencies are essentially correct. Qualitative analysis of the observed resonance Raman intensities indicates that the photoisomerization on the $\tilde{2}\ ^2B_1$ surface of the allyl radical proceeds by a disrotary process, in agreement with theoretical predictions. The Raman spectra indicate that the central CH bond does not directly photodissociate on the $\tilde{2}\ ^2B_1$ excited-state surface. Work is in progress on the perdeutero allyl-d_5 radical to confirm the assignments of the ν_6 and $2\nu_{12}$ features.

Acknowledgment. We gratefully acknowledge support for the work from the National Science Foundation (Grant 8923059), the National Institutes of Health (Grant 1P42-ES04699), and the Universitywide Energy Research Group of the University of California (Grant 444024). We thank Dr. Bruce Hudson of the University of Oregon and Dr. Jodye Selco of the University of the Redlands for helpful discussions.

Hemiacetal Anions: A Model for Tetrahedral Reaction Intermediates

Susan Baer, Elizabeth A. Brinkman, and John I. Brauman*

Contribution from the Department of Chemistry, Stanford University, Stanford, California 94305-5080. *Received April 6, 1990*

Abstract: A deprotonated hemiacetal ion is used as a model intermediate for nucleophilic addition reactions at a carbonyl group. The acidity of the cyclic hemiacetal 2-hydroxytetrahydropyran has been estimated to be $\Delta G°_{acid} \geq 351 \pm 2$ kcal/mol. The basicity of the deprotonated ion was found to be 347 ± 2 kcal/mol, different from the acidity by 4 kcal/mol. This difference is ascribed to an isomerization reaction in the ion. The electron affinity of the neutral radical corresponding to removal of an electron from the ion was measured with use of electron photodetachment spectroscopy and was found to be 49.6 ± 2.5 kcal/mol. The structure of the isomerized ion is assigned as a hydrogen bond stabilized enolate ion. The implications of the strong acidity of the hemiacetal for the stability of tetrahedral reaction intermediates are discussed. Thermochemical arguments suggest that tetrahedral adducts of this type are often global minima on the reaction potential surface. The addition reactions of different alkoxide–alcohol complexes with benzaldehyde are discussed in terms of the stability of the corresponding tetrahedral addition product.

I. Introduction

Nucleophilic carbonyl addition reactions play a critical role in a variety of chemical and biochemical processes, including enzyme-catalyzed hydrolysis of carboxylic acid derivatives. Due to their biological relevance, as well as their synthetic utility, carbonyl addition reactions have been extensively studied.[1] Studies of the reaction mechanism in solution suggest that the reaction proceeds through an intermediate tetrahedral structure where the oxygen carries the negative charge, as shown in eq 1.[2-6]

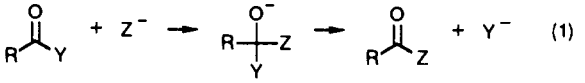

(1)

Scheme I

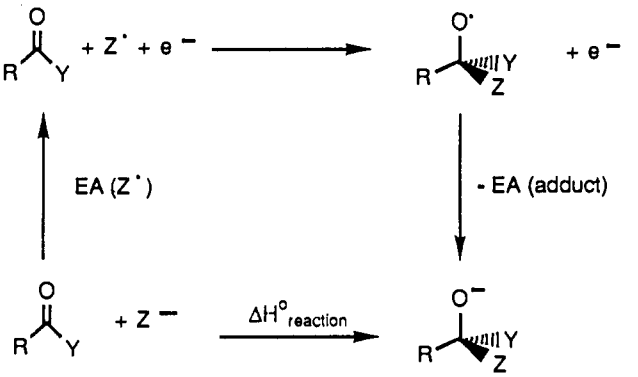

Nucleophiles	EA
CH_3^-	2 kcal/mol
CH_3O^-	37 kcal/mol
Cl^-	83 kcal/mol

This intermediate has been implicated in kinetic and isotope exchange experiments.[2a,3,4] In certain cases, direct spectroscopic evidence for its existence has been found.[5]

(1) March, J. *Advanced Organic Chemistry*; Wiley: New York, 1985; Chapters 10, 16.

(2) (a) Bender, M. L. *Chem. Rev.* **1960**, *60*, 53. (b) Bruice, T. C.; Benkovic, S. J. *Bioorganic Mechanisms*; Benjamin: New York, 1966; Vol. 1. (c) Patai, S., Ed. *The Chemistry of the Carbonyl Group*; Interscience, New York, 1966, 1970; Vol. 1, 2. (d) Jencks, W. P. *Acc. Chem. Res.* **1980**, *13*, 161. (e) Guthrie, J. P. *Acc. Chem. Res.* **1983**, *16*, 122.

(3) (a) Jencks, W. P. *Catalysis in Chemistry and Enzymology*; McGraw-Hill: New York, 1968; pp 463-554. (b) Johnson, S. L. *Tetrahedron Lett.* **1964**, 1481. (c) Johnson, S. L. *J. Am. Chem. Soc.* **1964**, *86*, 3819.

(4) (a) Bender, M. L.; Heck, H. A. *J. Am. Chem. Soc.* **1967**, *89*, 1121. (b) Bender, M. L.; Matsui, H.; Thomas, R. J.; Tobey, S. W. *J. Am. Chem. Soc.* **1961**, *83*, 4193. (c) Bunton, C. A.; Spatcher, D. N. *J. Chem. Soc.* **1956**, 1079. (d) Bender, M. L. *J. Am. Chem. Soc.* **1951**, *73*, 1626. (e) Bunton, C. A.; Lewis, T. A.; Llewellyn, D. H. *Chem. Ind. (London)* **1954**, 1154.

(5) (a) Capon, B.; Dosunmu, M. I.; de Nazaré de Matos Sanchez, M. *Adv. Phys. Org. Chem.* **1985**, *21*, 37. (b) Fraenkel, G.; Watson, D. *J. Am. Chem. Soc.* **1975**, *97*, 231. (c) Guthrie, J. P. *J. Am. Chem. Soc.* **1973**, *95*, 6999. (d) McClelland, R. H.; Santry, L. J. *Acc. Chem. Res.* **1983**, *16*, 394. (e) Tee, O. S.; Trani, M.; McClelland, R. H.; Seaman, N. E. *J. Am. Chem. Soc.* **1982**, *104*, 7219.

(6) (a) Fodor, G.; Letourneau, F.; Mandova, N. *Can. J. Chem.* **1970**, *48*, 1465. (b) Zaugg, H. E.; Popendick, V.; Michaels, R. J. *J. Am. Chem. Soc.* **1964**, *86*, 1339. (c) Woodward, R. B. *Pure Appl. Chem.* **1964**, *9*, 49.

0002-7863/91/1513-805$02.50/0